Striped-Pattern Deterioration and Morphological Analysis of Injection Moldings Comprising Polypropylene/Ethylene α-Olefin Rubber Blends. I. Influence of Ultraviolet Irradiation

Koki Hirano,[1,2] Satoshi Tamura,[1] Toshitaka Kanai[1–3]

[1]*Research and Development Division, Prime Polymer Company, Limited, 580-30 Nagaura, Sodegaura-City, Chiba 299-0265, Japan*
[2]*Division of Material Sciences, Graduate School of Natural Science and Technology, Kanazawa University, Kakuma-Machi, Kanazawa-City, Ishikawa 920-1192, Japan*
[3]*Research and Development Laboratory, Idemitsu Kosan Company, Limited, 1-1 Anesaki-Kaigan, Ichihara-City, Chiba 299-0193, Japan*

Received 3 October 2006; accepted 17 January 2007
DOI 10.1002/app.26332
Published online 8 May 2007 in Wiley InterScience (www.interscience.wiley.com).

ABSTRACT: Unique deterioration with a periodical striped pattern on the injection moldings of polypropylene/rubber blends is reported. After exposure to ultraviolet irradiation with a sunshine fade meter, striped patterns appeared on the injection moldings along the flow direction of the molten resin during the filling process of injection molding, even though the initial specimen showed no sign of any stripe pattern on its surface. The stripe was carefully observed with ultrasonic echo imaging, scanning electron microscopy, transmission electron microscopy, and Fourier transform infrared spectroscopy. As a result, a number of microvoids were observed inside the injected body at a depth of 50–100 μm from the surface. It became clear that the difference in the number of voids along the flow direction formed the stripe pattern. Surprisingly, these voids occurred in domains comprising a rubber phase. The distribution of voids in depth indicated the existence of a trace of a snakelike flow caused inside the injected body during the injection-molding process. © 2007 Wiley Periodicals, Inc. J Appl Polym Sci 105: 2416–2426, 2007

Key words: blends; injection molding; morphology; poly (propylene) (PP); rubber

INTRODUCTION

Polypropylene (PP) is one of the most widely used resins in the industrial field, not only in commodity equipment, packages, films, and electrical and home appliances but also in automotive applications.[1,2] PP is easily modified by the blending of rubber[3–7] and talc[8,9] to obtain higher performances for impact strength, rigidity, and dimensional stability, especially in automotive parts[10] such as bumper faces and instrumental panel garnishes. In the past 2 decades, PP blends have become the main materials for automotive parts for which good surface finishing is required as well as mechanical properties.

In general, these parts are manufactured by injection molding.

In the case of PP/rubber blends, it is well known that a periodically striped mark called a tiger stripe or flow mark occurs on the surface of the injection moldings from the gate side to the flow end, just about perpendicular to the flow direction of the molten resin.[11–14] Severe tiger striping sometimes spoils the surface finishing for paintless or partially painted parts. Previous studies have reported some mechanisms and measures to improve the tiger striping of PP/rubber blends in terms of numerical analysis[12] and morphology control.[11,13] Therefore, the stripe defect is not a severe issue for real automotive parts with appropriate designs making the stripe inconspicuous.[13–15]

Incidentally, light and weather resistance is also important for exterior applications because automotive cars are used outdoor for several years or more. It is well known that both UV irradiation and radiant heat derived from sunshine are key factors that induce severe deterioration of polymeric materials.[16] Moreover, rain water should be noted.

Even though a tiger stripe is inconspicuous in its initial state, in some cases the stripe is severely conspicuous after exposure to weather for a long time.[14]

Figure 1 shows typical striped-pattern deterioration of an injected bumper composed of PP/rubber blends (sample E in Table I) after exposure for a year in Okinawa Island, a southern part of Japan. A striped pattern formed by the alternation of strongly and weakly whitened parts can be easily seen by the naked

Correspondence to: K. Hirano (koki.hirano@primepolymer.co.jp).

Journal of Applied Polymer Science, Vol. 105, 2416–2426 (2007)

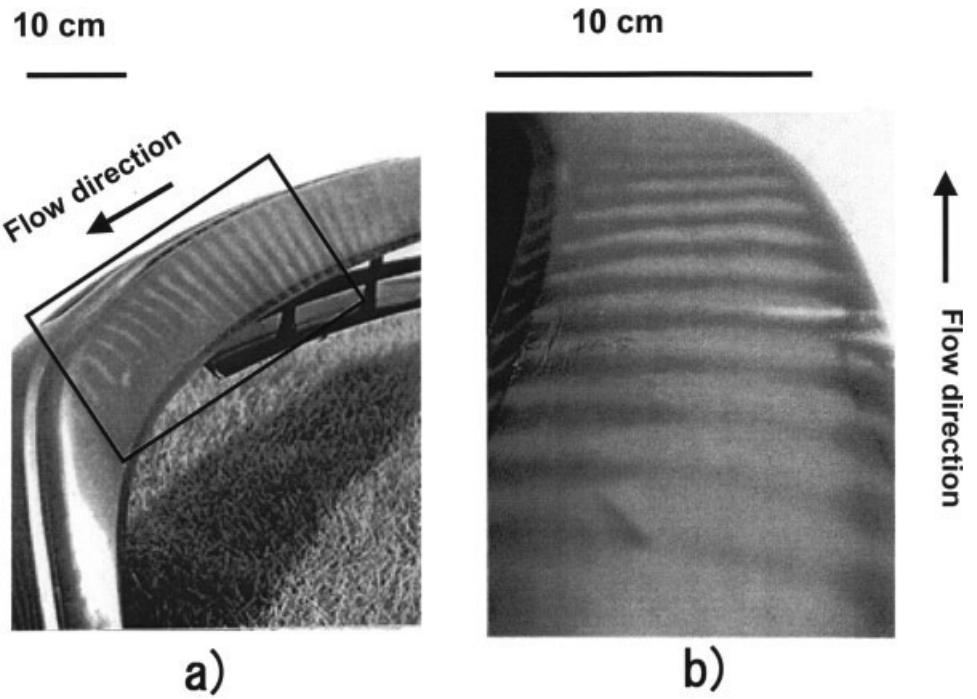

Figure 1 Typical patterns of the striped deterioration of real parts composed of the PP/rubber/talc blend (sample E) caused by outdoor exposure: (a) left half of the bumper and (b) macrograph of the bumper.

eye. The tiger stripe was not severe as in this photograph just after molding (in its initial state). However, both sunshine and weather induced such severe deterioration on the tiger-stripe pattern. In this sample, glossy (darkish) and cloudy (whitish) parts of the original tiger stripe became weakly and strongly whitened parts, respectively. Here this deterioration with a striped pattern was paid special attention.

Even if striped deterioration occurs, the mechanical properties, such as the flexural modulus and impact strength, do not become worse for mechanical requirements. In contrast, it becomes a serious defect for a surface-finishing design. Thus, striped deterioration is important in applications of PP/rubber blends for real use. However, any reports of striped deterioration have not been reported as far as we know. In this article, the morphological analysis of the stripe was carried out for model blends to estimate the mechanism of stripe deterioration.

EXPERIMENTAL

Materials

The PP resin used in this study was a high-impact copolymer with a 50 g/10 min melt flow rate (230°C, 2.16 kg); the 7 wt % rubber component of the propylene–ethylene copolymer was the *p*-xylene-soluble portion. It was catalyzed with a Ziegler–Natta catalyst system. This PP was manufactured by Prime Polymer Co., Ltd. (Tokyo, Japan). This PP is named bPP here because it was used as the base PP in this study. The ethylene α-olefin rubber was a metallocene-catalyzed ethylene butene copolymer named A-1050 (melt index = 1.2 g/10 min at 190°C, density = 0.87 g/cm^3) manufactured by Mitsui Chemical, Inc. (Tokyo, Japan). Talc named JM-209, having a 4 μm in average diameter according to a laser diffraction method, was supplied by Asada Mineral Co., Ltd. (Tokyo, Japan). Carbon black (CB) was a PP-based master pellet named P1-1070 from DIC, Inc. (Tokyo, Japan). The material combinations of the PP blends for UV irradiation are shown in Table I.

Sample preparation

The material formulations of the PP/rubber blends used here are shown in Table I. The blends were prepared with a 2FCM twin-screw compounding mixer (barrel diameter = 2 in.) from Kobe Steel, Ltd. (Hyogo, Japan), set at a barrel temperature of 200°C and a screw speed of 900 rpm. The productivity was 50 kg/h.

TABLE I
Formulations of the Blends Used in This Study (Parts by Weight)

Sample	bPP	Rubber	Talc	CB
A	100	—	—	—
B	90	—	10	—
C	70	30	—	—
D	63	27	10	—
E	63	27	10	0.6

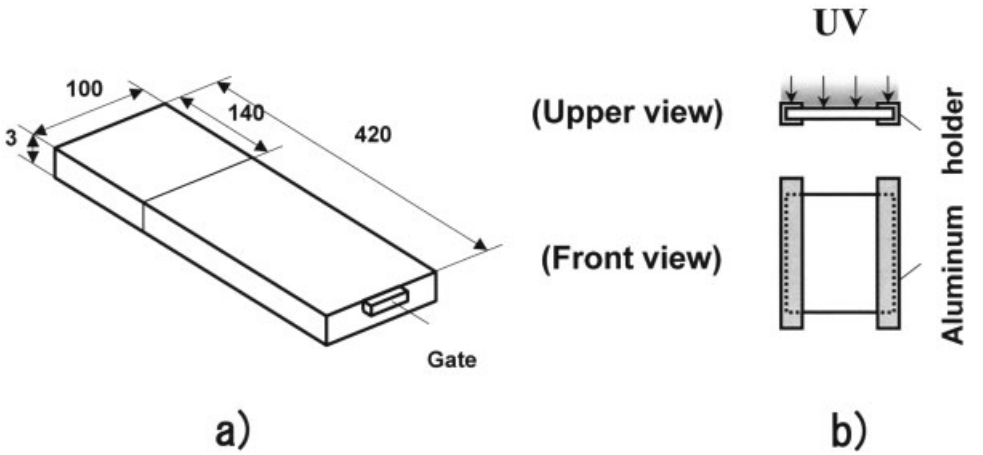

Figure 2 Schematic drawings of specimens used in this study: (a) dimensions (mm) of the injection plate and (b) attachment state for UV irradiation.

An antioxidant agent (1000 ppm), Irganox 1010 (Ciba Specialty Chemicals, Basel, Switzerland), was added to blends to prevent thermal degradation during this compounding process. In addition, a 1 : 1 (w/w) light-stabilizer mixture consisting of Tinuvin 770 and Tinuvin 120 (Ciba Specialty Chemicals) was added as an optional additive to confirm the effect of the light stabilizer. These blends were molded with an IS200CN injection machine manufactured by Toshiba Machine Co., Ltd. (Shizuoka, Japan), whose clamping force was 200 tons. The operating conditions were set at a cylinder temperature of 220°C and a filling time of 3.5 s. The specimen shape was a plate 420 mm long, 100 mm wide, and 3 mm thick. For UV irradiation, a 140-mm length of this specimen was cut from the flow end. The specimen dimensions and attachment state are shown in Figure 2.

UV irradiation

To obtain accelerated deterioration data, the sunshine fade meter used here was a WEL-SUN-HC (Suga Test Instruments Co., Ltd., Tokyo, Japan) operating at a black panel temperature of 83°C with a carbon-arc light source. The specimen set in the sunshine fade meter was supported on both sides by aluminum holders (Fig. 2). The region covered with these holders was not irradiated by UV.

Confocal laser scanning microscopy (LSM)

An LSM-GM (Olympus Corp., Tokyo, Japan) was operated under the following conditions: 20× magnification and 0.32 mm × 0.48 mm for the view. Both the brightness and roughness used here were obtained by an analysis of the reflected light from the surface.

Ultrasonic echo imaging

A UH Pulse 100 ultrasonic reflectscope (Olympus) was used. The measurement was carried out through water under the following conditions: an 8-mm^2 scanning zone and a frequency of 30 Hz. The limit of detection size and the maximum penetration thickness were about 20 μm and 10 mm, respectively, according to the manufacturer.

Morphology observation with electron microscopy

The morphologies were observed with a JEOL JSM-6100 scanning electron microscope and a JEOL JEM-1010 transmission electron microscope (JEOL Ltd., Tokyo, Japan). The cross section for scanning electron microscopy (SEM) was prepared by an ultramicrotome from the sample embedded with the epoxy resin. Sliced specimens for transmission electron microscopy (TEM) were prepared with a microtome and were dyed under RuO_4 vapor.

After binarization, TEM photographs were analyzed statically with image analysis to evaluate the morphology of the dispersed phase in terms of the particle size and orientation.

Fourier transform infrared (FTIR) spectroscopy

An FTS6000 spectrometer and a UMA 500-μm unit manufactured by Varian, Inc. (Bio-Rad, CA), were

TABLE II
Formulation Dependence of the Deterioration Pattern Caused by UV Irradiation

Sample	bPP	Rubber	Talc	CB	Deterioration pattern
A	O	—	—	—	No stripe
B	O	—	O	—	No stripe
C	O	O	—	—	Stripe
D	O	O	O	—	Stripe
E	O	O	O	O	No stripe (not deteriorated)

The black panel temperature was 83°C, the light source was the carbon arc, and there was no rain. O = ingredient in the sample; — = ingredient not in the sample.

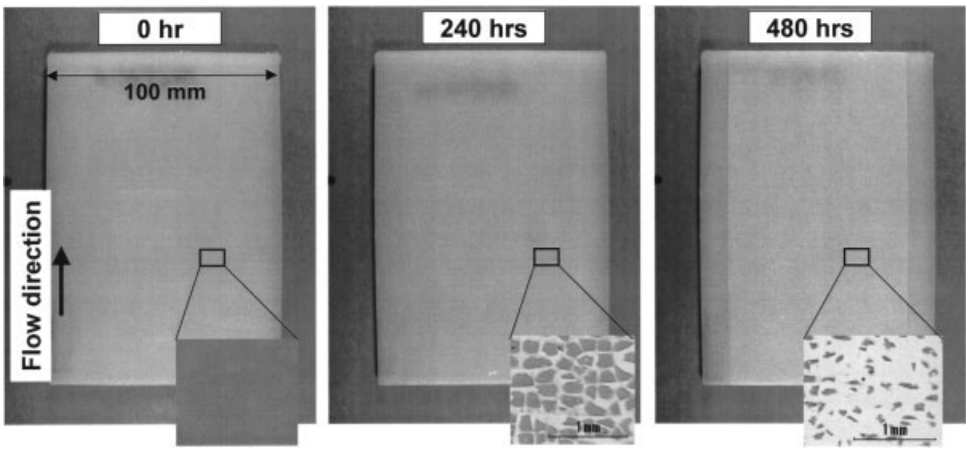

Figure 3 Photographs of the bPP (sample A) dependent on the UV-irradiation time.

operated with the total reflection method, in which a germanium prism and a 250-μm^2 aperture were adopted. The specimen was sliced with a razor by hand before the measurements.

RESULTS AND DISCUSSION

Dependence of the deterioration pattern on the material formulation

The results of the UV-irradiation experiments are summarized in Table II. Sample A (bPP) and sample B (bPP/talc) did not indicate any stripe pattern after irradiation for 2000 h. In these samples, unified deterioration with microcracks on the surface occurred. This deterioration pattern is well known as the general pattern caused by UV irradiation to PP. On the other hand, sample C (bPP/rubber) and sample D (bPP/rubber/talc) indicated severe stripe patterns that could be recognized easily by the naked eye. In addition, no striped pattern was detected in sample E (PP/rubber/talc/CB) after 4000 h of irradiation. It is well known that CB acts on a UV absorber, so we estimated that sample E containing CB indicated good resistance to UV irradiation. Here, the model blends that did not contain CB are discussed. Model blends that caused striped-pattern deterioration were samples C and D. Both contained bPP and rubber. Therefore, these two ingredients are keys for providing striped deterioration.

The appearances of samples A and C, dependent on the irradiation time, are compared in Figures 3 and 4, respectively. No striped pattern was observed in the original specimen before UV exposure for both samples A and C by the naked eye or a confocal scanning laser microscope, as mentioned later in Figure 7. In sample A, the surface roughness increased with increasing elapsed time. This result was explained in terms of microcrack growth, which is shown in the macrophotograph of Figure 3. This was general deterioration for PP.[17] In contrast to sample A, a striped pattern developed on sample C with increasing irradiation time. This stripe was formed by the alternation of strongly and weakly whitened parts (indicated as S

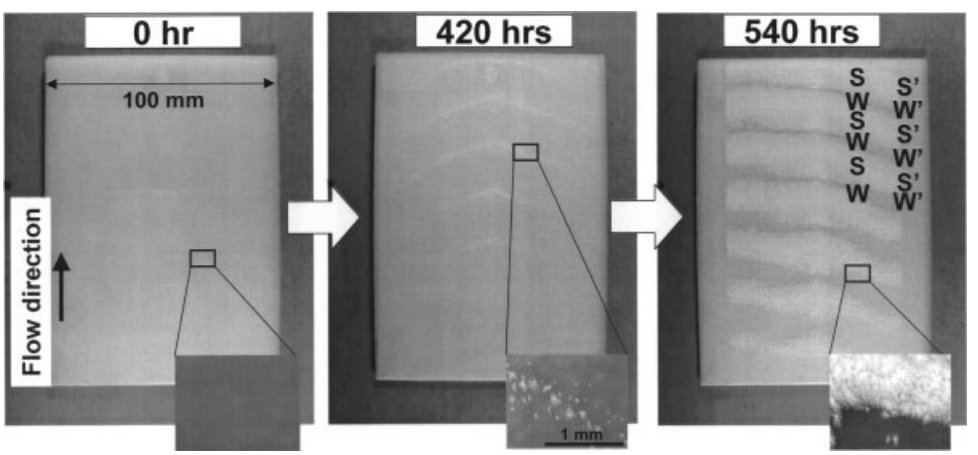

Figure 4 Photographs of the PP/rubber binary blend (sample C) dependent on the UV-irradiation time.

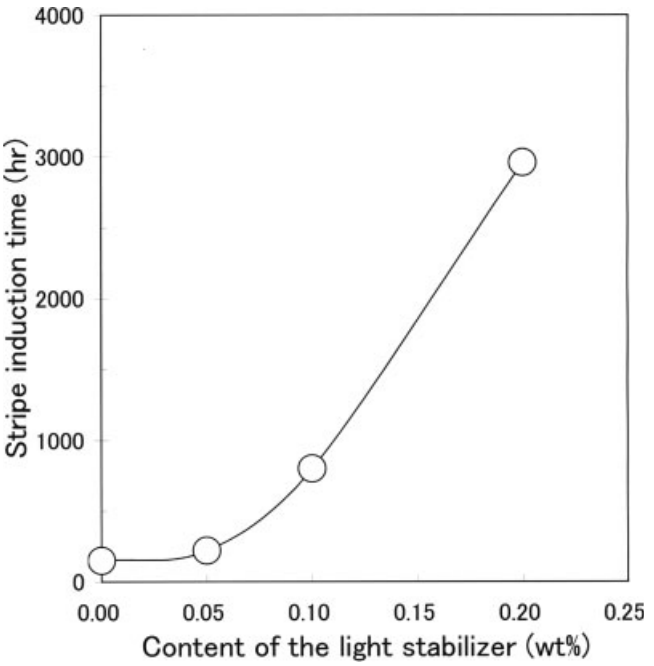

Figure 5 Induction time of the deteriorated stripe versus the light stabilizer content (sample C).

and W, respectively, in Fig. 4). The macrophotograph shows that small, whitened domains occurred with irradiation. Moreover, a number of these whitened domains became dense with increasing irradiation time, especially in the strongly whitened part. A similar stripe was observed on sample D.

Effect of the light stabilizer

For sample C (PP/rubber binary blend), the effect of the light stabilizer was confirmed on the basis of the content dependence of the stabilizer (Fig. 5). With increasing stabilizer content, the induction time of the deteriorated stripe clearly increased. Here, it was defined as the time at which narrow whitened lines approximately perpendicular to the flow direction (just like a pinstripe) were first detected by regular daily checking during the exposure experiments. This result was very important because of the distinct evidence that indicates the deteriorated stripe was controlled by UV but not the thermal history during the UV-exposure experiment. The effect of CB mentioned previously was also evidence.

Stripe-type deterioration of a PP/rubber binary blend as a model blend

To simplify the analyses, sample C (the bPP/rubber binary blend) was carefully examined by means of several physical methods.

It was necessary to determine where the striped deterioration occurred in the binary blend. In some previous studies,[11,14] including our article on the tiger stripe, it was able to be described with an optical method, such as gloss.

Before the discussion, the tested sample is confirmed again in Figure 6, which presents a schematic view of the deterioration of sample C as shown in Figure 4. The irradiated specimen provided severe striping, but the stripe did not develop to both edge sides of the plate because these edges were not irradiated with UV on account of the aluminum holders that supported the plate on its edges during the irradiation test (Fig. 2). These edge sides could sustain the original state of the injection-molding plate without the irradiation. If the edge sides had been irradiated with UV, striped deterioration should have been caused. The parts just adjacent to S and W are defined as S′ and W′, respectively. S′ and W′ become S and W, respectively, by irradiation. Thus, we were able to confirm the influence with or without UV on the deterioration.

Here, the deteriorated stripe of sample C was characterized for its surface by means of confocal LSM, which could provide the brightness and roughness of a specimen's surface. Figure 7 shows the surface properties obtained with LSM. Both the brightness and surface roughness are plotted to the position along the flow direction. The original part (nonirradiation area) indicated higher brightness and lower roughness. It was clarified that the surface of the original plate had a smooth surface on the basis of these data.

On the other hand, the irradiated part indicated lower brightness and higher roughness in comparison with the original part. This meant that the irradiation made the surface entirely rough by UV deterioration.

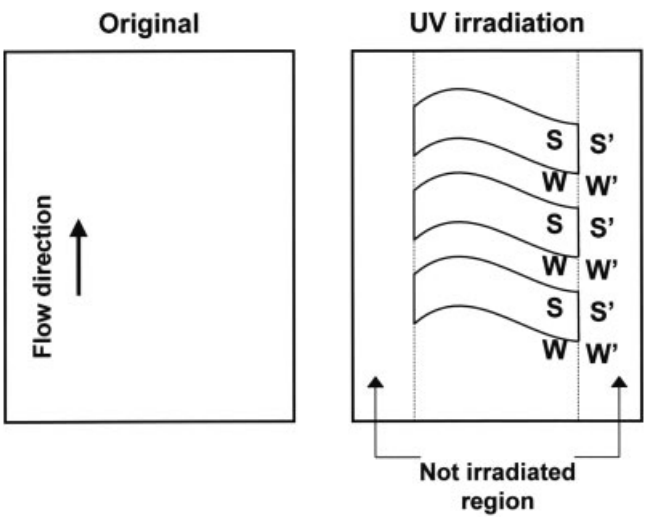

Figure 6 Definitions of the stripes caused by UV irradiation: S is the strongly whitened part; W is the weakly whitened part; and S′ and W′ are the unirradiated areas on the extension of S and W, respectively.

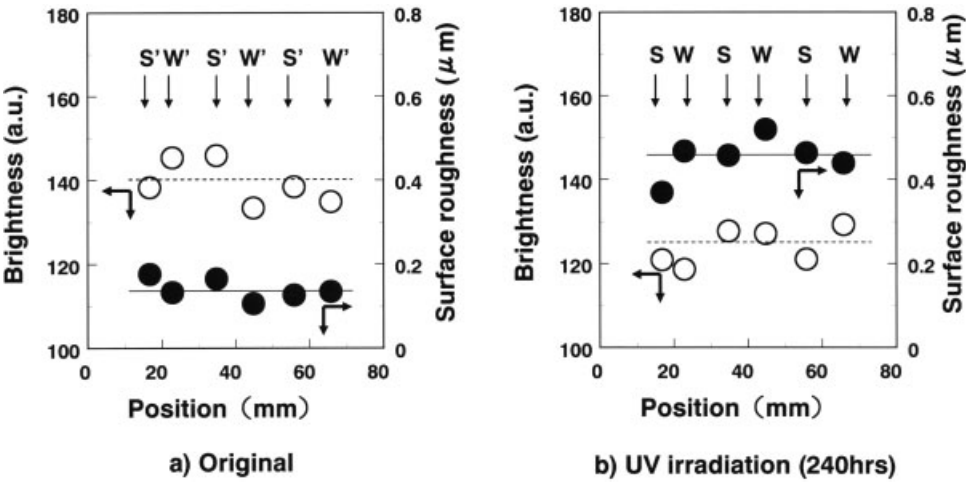

Figure 7 Results of surface analyses with a confocal scanning laser microscope.

Incidentally, the data varied with the position, but no periodical change corresponding to S′ and W′ or S and W was observed. These variations of the data were allowable errors in the LSM apparatus. This result is important. Even though the conspicuous stripe was developed on the irradiated area, no striped traces were observed on the surface. The striped deterioration of the PP/rubber binary blend caused by UV irradiation did not exist on the surface. Where did the striped deterioration form?

For more discussion, ultrasonic echo imaging was performed. This method is able to provide the internal structure according to the reflection and interference of ultrasonic echos.[18] Figure 8 shows the imaging of sample C before and after irradiation. For the original (before irradiation), the entire view was black. This result indicated that no hollow structures existed inside the original plate. In contrast to this result, for the UV-irradiated plate, white-spotted regions were observed partially against a black background. These white-spotted regions corresponded to some hollow structures inside the irradiated plate. The spotted region increased and grew with the time of UV irradiation, and it was large in the S part versus the W part. As mentioned later, these spotted regions were formed by the aggregation of microvoids inside the specimen.

Abdel-Bary et al.[19] studied the UV deterioration of PP/rubber blends in films, but no results regarding hollow structures caused inside were reported. Therefore, this result obtained in our experiments is a unique phenomenon in injection moldings composed of a PP/rubber blend.

Influence of oxidation on chemical deterioration

As is generally known, UV induces the scission of a polymer chain of PP on the basis of a β-oxidation process.[16] As evidence of oxidative deterioration, the production of carbonyl group (C=O) is often used to describe the degree of oxidation.[20,21] Here, the C=O content was measured in the striped deterioration

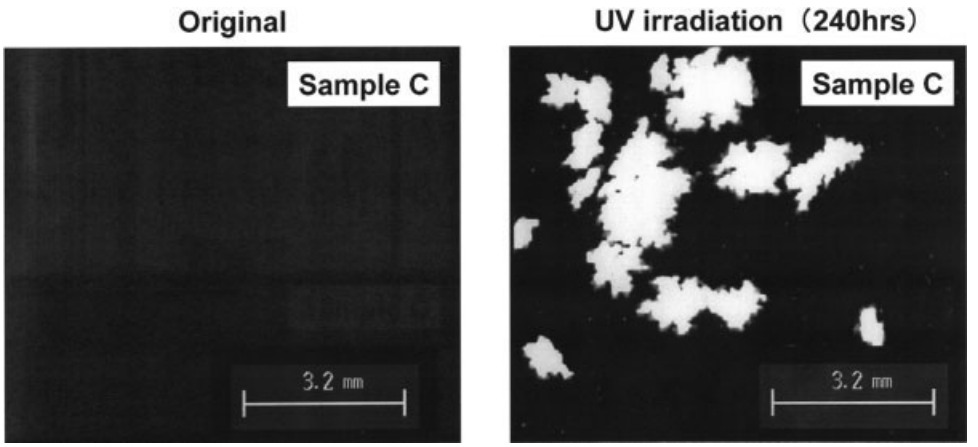

Figure 8 Ultrasonic echo imaging of the whitened part in the striped deterioration.

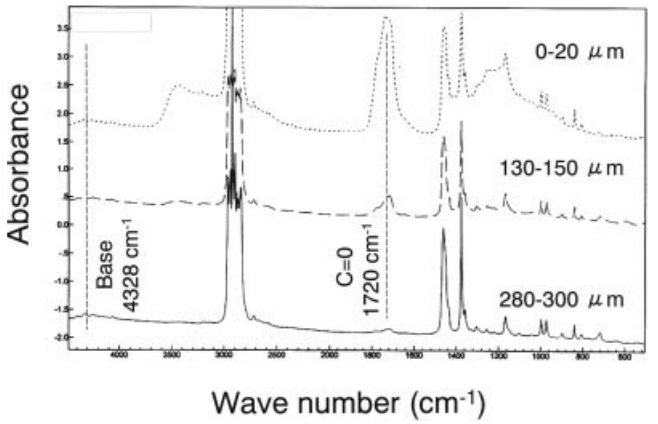

Figure 9 Depth-profile FTIR spectra of the deteriorated part (weakly whitened part of sample C after UV irradiation for 420 h).

plate of sample C to discuss the influence of the chemical deterioration on the stripe caused by UV irradiation.

Figure 9 shows a set of FTIR spectra dependent on the depth from the surface to the inside. The peak of 1720 cm^{-1} is assigned to C=O. The absorbance ratio of the C=O index is defined as the ratio of the peak intensity for 1720 cm^{-1} to that for 4328 cm^{-1}. The C=O index was strongest at the surface, and it decreased with increasing depth. It is clear that the peak intensity of C=O is strong at the surface.

The depth profile of the C=O index of the striped deterioration is shown in Figure 10. Two profiles for the S part and W part are compared in this figure. Here, the generations of C=O were almost the same between the S and W parts. The surface was mostly deteriorated in comparison with the inside of the specimen in terms of chemical deterioration.

Therefore, the chemical deterioration (C=O produced by oxidation) could not directly provide this striped deterioration because a significant difference in the C=O contents was not observed in both S and W through the depth.

Position at which the hollow structures occurred

The result of the ultrasonic echo imaging shows that some hollow structures occurred inside the specimen of the PP/rubber binary blend after UV irradiation. To confirm where the hollow structure occurred, SEM observations were performed. The SEM photographs of the cross sections of the striped deterioration parts are shown in Figure 11. Here, the number of microvoids can be easily seen. Hollow structures (microvoids) certainly existed inside the injection molding in which the striped deterioration was caused, as the ultrasonic echo experiment indicated.

These cross-section specimens were not treated with any solvent that acted as an etching agent. Therefore, these voids were not caused by the dissolution of any components contained in the sample.

The microvoids occurred at about a 20–140-μm depth from the surface. In the S part, the voids existed in a shallow region. On the other hand, in the W part, the voids existed in a deeper region. The depths in which the microvoids were generated differed in these two parts of the deteriorated stripe.

In addition, no voids were observed at the surface, including extremely near the surface region. This result supported the idea that the surface

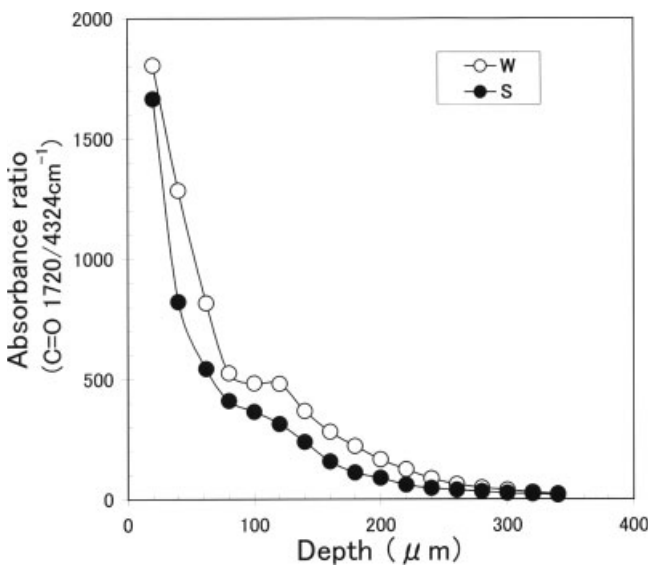

Figure 10 Depth profile of the carbonyl group (S is the strongly whitened part, and W is the weakly whitened part). Sample C after UV irradiation for 420 h.

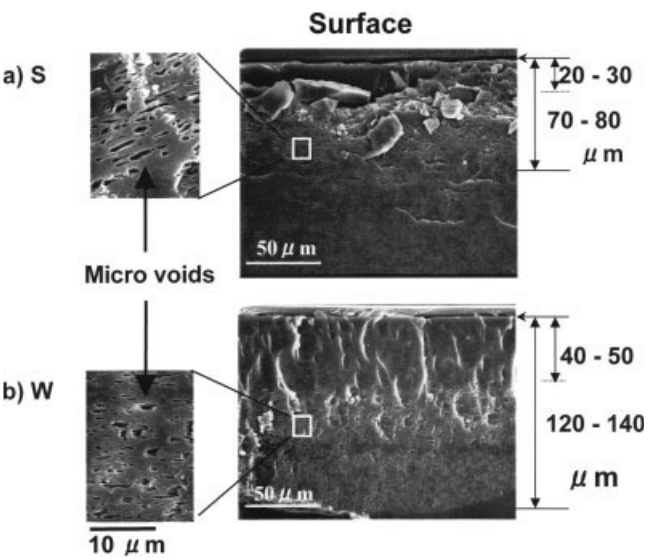

Figure 11 SEM photographs of the deteriorated stripe near the surface of sample C after UV irradiation for 420 h.

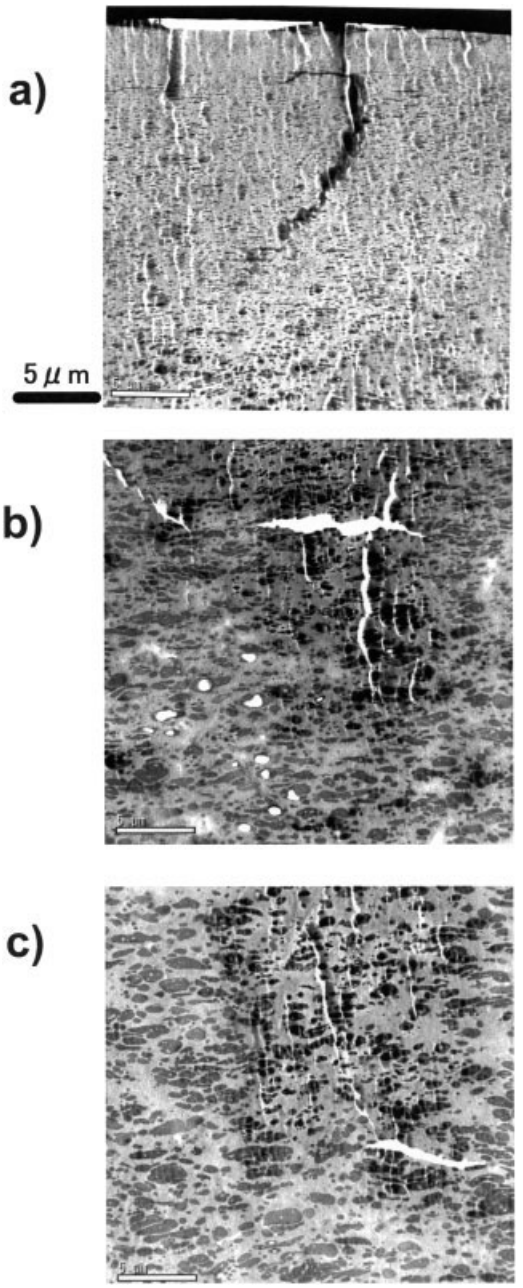

Figure 12 TEM photographs of the cross sections of a deteriorated stripe on sample C after UV irradiation for 240 h: (a) 0–20-μm depth, (b) 30–50-μm depth, and (c) 90–110-μm depth.

showed uniform properties in the brightness and roughness obtained with LSM in the S and W parts (Fig. 7).

Thus, it was confirmed that UV irradiation caused the microvoids inside the injection molding composed of the PP/rubber binary blend.

As shown in Figure 10, the profile of the C=O index looks like a plateau region at a depth of about 100 μm. This depth is close to the one at which the microvoids occur.

Place in which the microvoids were generated

It is well known that a PP/rubber binary blend system has a multiphase in terms of the morphology: a homo-PP portion as the continuous phase (the matrix), a rubber portion as the dispersed phase (the domain), and an interface between the matrix and the domain. It is very interesting and important where the microvoids caused by UV irradiation occur in this PP/rubber binary blend system in view of the photodeterioration for a multiphase system of the polymer blend.

To discuss this on the basis of the multiphase morphology, TEM observations were performed. Figure 12 shows TEM photographs of sample C (0.05 wt % light stabilizer) after UV irradiation for 240 h. The specimen was irradiated for a longer time; it had many microvoids inside it and was too brittle to prepare an ultrathin film for TEM observation. Then, the 240-h specimen was used. In this figure, three points in the depth are shown. Some cracks appear in the photographs. They were caused by the operation with a glass knife because the specimen was brittle according to the irradiation.

In these photographs, the dark domains are assigned to the dispersed rubber phase. At the region near the surface (0–20 μm), the domain size is relatively small and highly orientated along the flow direction. In the shallower region (30–50 μm) and the deeper region (90–110 μm), the domain size is relatively large and moderately orientated.

Incidentally, where do the microvoids exist? The void can be seen in only the shallower region [Fig. 12(b), 30–50 μm], especially on the left and underside of the photograph. The other two regions do not have any microvoids, except for the cracks caused by the glass-knife operation.

A macrophotograph of the microvoids is shown in Figure 13, in which the original part (not irradiated) is

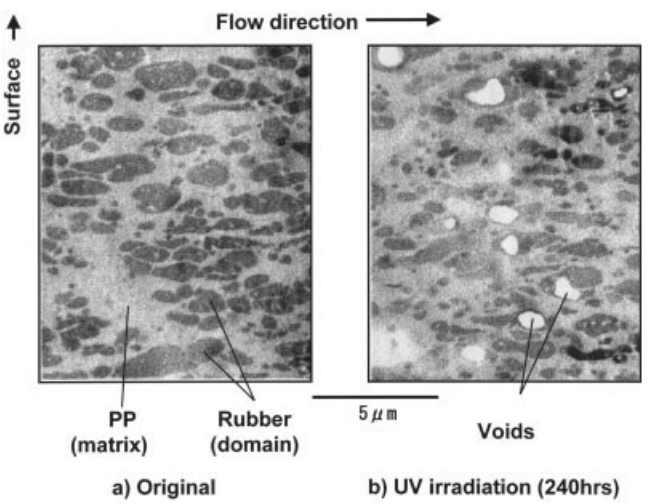

Figure 13 Expanded view of the TEM images of sample C at a 40–60-μm depth after UV irradiation for 240 h.

TABLE III
Results of Morphological Analysis Using Binarized Images (Sample C, 240 h)

Region		Depth (μm)	Particles (number/100 μm^2)	Average size (μm)	Aspect ratio
S′	MD–ND	30–50	804	2.9	7.4
		90–110	599	3.3	4.5
		150–170	592	3.8	4.6
	TD–ND	40–50	1251	1.7	2.1
		50–70	1355	1.9	1.9
		150–170	996	2.3	2.0
W′	MD–ND	30–50	916	3.9	14.0
		70–90	719	3.2	4.4
		170–190	583	4.8	6.2
	TD–ND	40–50	1161	2.0	2.4
		100–120	847	2.3	2.2
		200–220	1135	2.3	2.0

also shown. The typical matrix–domain structure can be seen for the original specimen. The photograph of the irradiated one clearly indicates that microvoids were generated. In attention, all the voids observed here are surrounded by a dark portion. As mentioned previously, the dark portion is the rubber phase. Therefore, the voids are generated not at the PP matrix or the interface but just inside the dispersed rubber domain. It is a very interesting result as we know. It was confirmed that the rubber used in this study (the ethylene butene copolymer) is not apt to deteriorate by UV in comparison with PP on the basis of the UV-irradiation experiment in which either the rubber or PP was examined independently. The measurements of the C═O index of the surface using FTIR provided the following results: 1090 ppm for bPP, 454 ppm for the PP/rubber, and 27 ppm for the rubber after UV irradiation for 220 h at a black panel temperature of 63°C. Moreover, the domains having higher orientation near the surface of the specimen did not have any microvoids inside, even though the surface was directly exposed by UV.

Relationship between the striped deterioration and internal structures of the PP/rubber binary blends

It seems that the depth at which the microvoids occurred was strongly influenced by the dispersed phase morphology rather than the strength of C═O generation. Then, the morphological distribution for the strongly whitened and weakly whitened parts was evaluated. Binarized image data of the TEM photographs were used for the image analysis. The domain size and orientation were obtained along the depth (Table III). Both the S′ and W′ regions (unirradiated region) were used for this analysis.

Figure 14 shows the average diameter and aspect ratio of the dispersed rubber domain along the depth. This morphological analysis was performed for the two cross sections MD–ND and TD–ND, where MD is the machine direction (flow direction), TD is the transverse direction of the flow, and ND is the normal direction. After binarization, hundreds of domains or more were evaluated for the image analysis with ana-

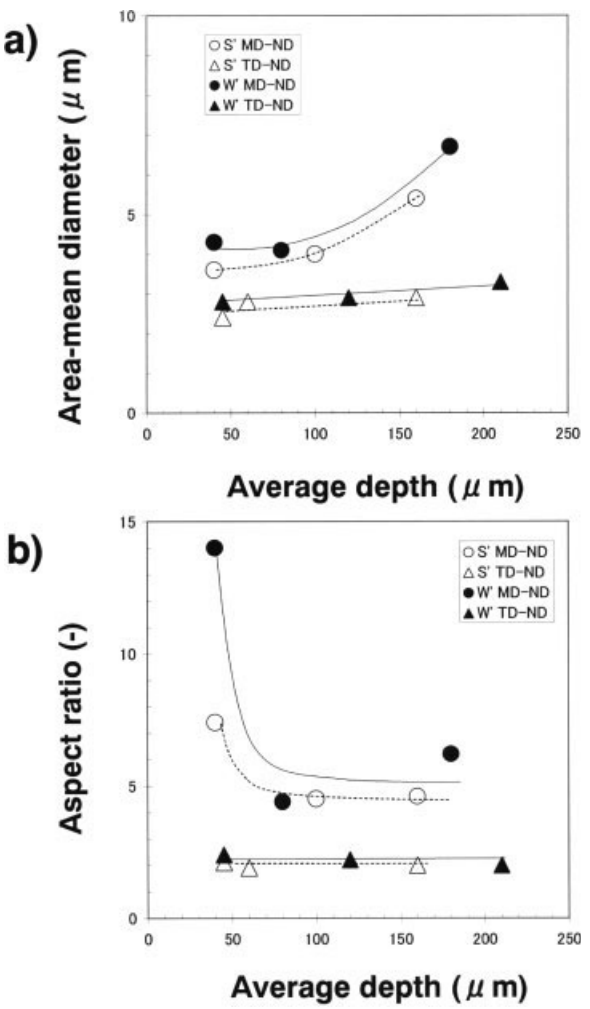

Figure 14 Morphological analyses of the dispersed rubber phase with binarized images of TEM photographs of sample C: (a) depth dependence of the average length and (b) depth dependence of the aspect ratio.

lytical software named NIH Imaging, which approximates the domain shape to a corresponding ellipsis shape. Here the length of the long axis of the ellipse was adopted as the average diameter for the morphological analysis; the following equation provides the diameter known as the area-mean diameter:

$$\text{Average diameter} = \frac{\sum x_i^3}{\sum x_i^2} \quad (1)$$

where x_i is the length of the long axis of the domain having an index of i. Also, the aspect ratio of the length of the long axis and that of the short axis of the ellipse was obtained to describe the degree of orientation of the dispersed rubber.

The average size increased with increasing depth, but it did not indicate a significant difference between S′ and W′ for both MD–ND and TD–ND. On the other hand, the aspect ratio dependent on the depth differed in S′ and W′ for their MD–ND cross sections. Figure 14(b) shows the data. A deeper region from the average depth of 100 μm did not indicate distinct difference in the aspect ratio of the dispersed rubber phase for both MD–ND and TD–ND cross sections. However, a shallower region near the surface of the injection molding indicated that the aspect ratio of W′ was higher than that of S′. It was a significant difference because hundreds of the particles (dispersed rubber phase) were used for the statistical analysis of imaging. These data show that the dispersed rubber is highly oriented along the flow direction (MD) with a rodlike shape near the surface. Moreover, the orientation of rubber develops more deeply for the W′ part than for the S′ part. Therefore, the boundary depth between the oriented rubber region having the higher aspect and the elliptical rubber region having the lower aspect is shallower in the W′ part than the S′ part. Generally, this boundary is for the shear zone and core zone in injection moldings composed of a PP/rubber blend.[22]

A more highly oriented rubber domain develops to a deeper position for the W part, and it does not cause microvoids after UV irradiation.

Morphological analysis and evidence of snakelike flow

Finally, we obtained a morphological schematic view (Fig. 15).

Highly oriented rubber domains exist in a shallow region from the surface. Under this zone having a highly oriented rubber domain, weakly oriented rubber domains exist. UV irradiation causes microvoids inside these weakly oriented rubber domains. In the S part, the thickness at which the highly oriented rubber domains exist is thin. Therefore, the microvoids are generated in the shallower position in comparison with the W part. As shown in Figure 7, the surfaces did not have any striped pattern but instead had a smooth surface. Of course, these two parts are adjacent to each other along the flow direction. These results show that a trace of a snakelike, unstable flow was recorded under the smooth surface.

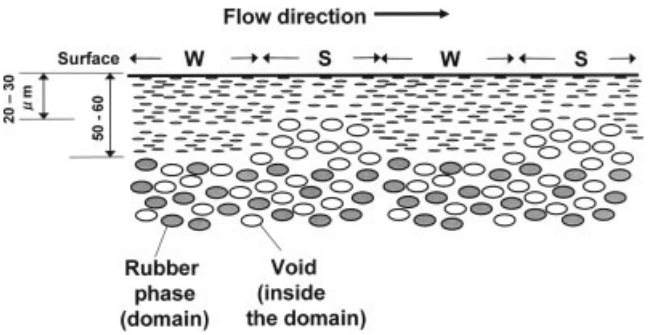

Figure 15 Schematic drawing of the striped deterioration of the PP/rubber binary blend.

When a conspicuous tiger stripe (flow mark) is not observed on the surface of an injection molding composed of a PP/rubber blend, the trace of the unstable flow is occasionally recorded and is able to generate surface-finishing defects during exposure to weather conditions.

CONCLUSIONS

In this study, we report unique deterioration having striped pattern for PP/rubber binary blends caused by UV irradiation. The striped deterioration was carefully analyzed with analytical methods, such as laser microscopy, ultrasonic imaging, FTIR, SEM, and TEM, including image analysis. The obtained results can be summarized as follows:

1. UV causes striped deterioration on an injection molding composed of PP/rubber blends.
2. The deteriorated stripe consists of microvoids caused inside the injection molding and is not on the surface. The difference in the depths at which the microvoids occur provides a stripe having alternating strongly whitened and weakly whitened parts approximately perpendicular to the flow direction. The depth generating the voids is shallow for the strongly whitened part and deep for the weakly whitened part. The location at which the microvoids occur has been consequently confirmed; the weakly oriented rubber domains under the zone having highly oriented rubber near the surface generate the voids inside themselves, whereas the highly orientated rubber near the surface does not have the void inside itself.
3. A trace of the snakelike, unstable flow during the injection process occasionally exists under the

smooth surface of the injection molding and becomes striped deterioration by UV exposure.
4. Chemical oxidation by UV does not directly provide the reason why the voids are caused in the deeper region from the surface, even though the surface is mostly oxidized.

Some trial studies involving the mobility of the segmental motion of the rubber domain and finite element method (FEM) analysis of the matrix–domain system for PP/rubber binary blends are being examined by the authors.

The authors gratefully thank Dr. A. Torikai for her advice on the deterioration of polyolefins. Mr. S. Ikeuchi kindly assisted with the electron microscopy observations and analysis. Finally, Prime Polymer Co., Ltd., is gratefully acknowledged for permitting us to release this study.

References

1. Moore, E. P. Polypropylene Handbook; Hanser Gardner: Cincinnati, 1996.
2. Polypropylene: An A–Z Reference; Karger-Kocsis, J., Ed.; Kluwer Academic: Dordrecht, The Netherlands, 1999.
3. Liang, J. Z.; Li, R. K. Y. J Appl Polym Sci 2002, 77, 409.
4. D'Orazio, L.; Marcarella, C.; Martuscelli, E.; Polato, F. Polymer 1991, 32, 1186.
5. van der Wal, A.; Nijihof, R.; Gaymans, R. J. Polymer 1999, 40, 6031.
6. Walton, K. L. Rubber Chem Technol 1996, 77, 3523.
7. Wu, G.; Nishida, K.; Takagi, K.; Sano, H.; Yui, H. Polymer 2005, 45, 3085.
8. Obata, Y.; Sumitomo, T.; Ijitsu, T.; Matsuda, M.; Nomura, T. Polym Eng Sci 2001, 41, 408.
9. Maiti, S. N.; Sharma, K. K. J Mater Sci 1991, 27, 4605.
10. Maxwell, J. Plastics in the Automotive Industry; Wood Head: Cambridge, England, 1994.
11. Patham, B.; Papworth, P.; Jayaraman, K.; Shu, C.; Wolkowicz, M. D. J Appl Polym Sci 2005, 96, 423.
12. Grillet, A. M.; Bogaerds, A. C. B.; Peters, G. W. M.; Baaijens, F. P. T. J Rheol 2002, 46, 651.
13. Hirano, K. Idemitsu Tech Rep 2005, 48, 124.
14. Hirano, K.; Suetsugu, Y.; Kanai, T. J Appl Polym Sci 2007, 104, 192.
15. Nakagawa, M.; Hirano, K.; Obata, Y.; Sugita, Y.; Nomura, T.; Matsuda, M.; Iwai, H.; Nagai, T. U.S. Pat. 6,667,359.
16. Rabek, J. F. Photodegradation of Polymers—Physical Characteristics and Applications; Springer: Berlin, Germany, 1996.
17. Rabello, M. S.; White, J. R. Polym Compos 1996, 17, 691.
18. McMaster, R. C., Nondestructive Testing Handbook; Ronald: New York, 1959.
19. Abdel-Bary, E. M.; Abdel-Razik, E. A.; Abderaal, M. Y.; El-Sherbiny, I. M. Polym Plast Technol Eng 2005, 44, 837.
20. Zweifel, H. Chimica 1993, 47, 390.
21. Carlsson, D. J.; Wiles, D. M. Macromol 1971, 4, 174.
22. Zhong, G.-J.; Li, Z.-M. Polym Eng Sci 2005, 45, 1655.